Hydrothermal carbonization of native African elemi shell (*Canarium schweinfurthii*) for porous hydrochar production and characterization for CO_2 capture

Calistus Princewill Odeh[1]*, Chinedu Ogonna Mgbemena[2], Orobosa Kingsley Osazuwa[1], Uchanna Ekene Okaforobah[1], Chukwubuikem Pascal Onyia[1]

[1]Nnamdi Azikiwe University, Awka, Anambra State, Nigeria

[2]Federal University of Petroleum Resource Efurun, Delta State, Nigeria

*Corresponding author, email: cp.odeh@unizik.edu.ng

Article history

Submitted: 10 August 2026

Revised: 15 September 2026

Accepted: 29 September 2026

Published: 4 October 2025

Keywords

Biomass

Capture

Carbonization

Hydrochar

Pore volume

Abstract

This study investigated the valorization of African elemi shell (*Canarium schweinfurthii*) as a renewable feedstock for hydrochar production through hydrothermal carbonization (HTC). Response Surface Methodology based on Central Composite Design was used to evaluate the effects of reaction temperature, residence time, and water-to-biomass ratio on hydrochar textural properties. The hydrochars were characterized using BET/BJH analysis, ultimate and proximate analyses, SEM–EDS, FTIR, and TGA/DTA. Increasing reaction temperature and residence time generally enhanced pore development, with the highest measured surface area and pore volume reaching 1073.93 m^2/g and 0.35 cm^3/g, respectively, at 220 °C, 90 min, and a W–B ratio of 12. The carbon content also increased substantially after HTC, reaching 88.27% at 220 °C, compared with 54.79% for the raw shell. FTIR analysis confirmed structural transformation and the presence of functional groups associated with the carbonized material, while TGA/DTA revealed altered thermal decomposition behaviour following HTC. Overall, the results demonstrate that African elemi shell can be effectively converted into a carbon-rich, porous hydrochar with favourable textural and chemical characteristics, indicating its potential for CO_2 capture and other environmental applications.

1. Introduction

The transformation of industrial and agricultural biomass residues into value-added products such as hydrochar and biochar has attracted considerable research interest due to the increasing need for low-cost, renewable, and environmentally sustainable carbonaceous materials. This interest is further driven by global environmental challenges, including the continuous rise in carbon dioxide (CO_2) emissions, climate change, and pollution arising from industrial and agricultural activities [1]. Biomass-derived carbon materials have considerable potential for applications in energy technologies, environmental remediation, pollution control, and carbon sequestration because of their renewable origin, relatively low production cost, and environmental benefits [2]. The nature and composition of the biomass feedstock play an important role in determining the structural, chemical, and functional properties of the resulting biochar and hydrochar. Biomass resources such as forestry residues, animal wastes, municipal organic materials, and agricultural by-products are particularly attractive feedstocks because their carbon-rich constituents can contribute to the production of high-quality carbon materials [3].

Among the thermochemical technologies employed for the conversion of biomass into carbonaceous products, pyrolysis and hydrothermal carbonization (HTC) are among the most widely investigated processes [4]. Hydrothermal carbonization is particularly advantageous for biomass with high moisture content because the process can be conducted directly in an aqueous medium without the need for extensive and energy-intensive preliminary drying. The process generally operates at moderate temperatures, typically within the range of 180–260 °C, and under the corresponding autogenous pressures required to maintain the reaction medium in the liquid phase [5]; [6]. During HTC, biomass undergoes a series of physicochemical transformations involving hydrolysis, dehydration, decarboxylation, fragmentation, polymerization, and condensation. These reactions result in the formation of hydrochar as the major solid product, together with bio-oil and small quantities of gaseous products [7]. Because a considerable proportion of the original carbon and energy contained in the biomass can be retained in the solid phase, hydrochar has emerged as a promising material for carbon management, particularly in CO_2 adsorption and carbon capture applications [8];[9].

The properties and performance of hydrochar are strongly influenced by the conditions under which HTC is carried out. Important operating variables include reaction temperature, residence time, water-to-biomass ratio, characteristics of the feedstock, and the presence or absence of catalysts. These parameters influence the

© 2026 The Author(s)
This work is licensed under a Creative Commons Attribution-ShareAlike 4.0 International License
ISSN: 3110-1577

extent of biomass decomposition and consequently determine important hydrochar characteristics such as product yield, carbon content, surface area, pore volume, and pore-size distribution [10]. Although hydrochar obtained directly from HTC may possess a relatively low specific surface area and limited microporosity, its textural and adsorption properties can be substantially improved through appropriate optimization of the HTC conditions and subsequent activation or post-treatment processes [11]. Such improvements are particularly important when the hydrochar is intended for gas adsorption, where the development of suitable pore structures and surface-active sites is essential for effective CO_2 uptake.

African elemi (*Canarium schweinfurthii*) is a tropical tree widely distributed across parts of West and Central Africa, including Nigeria, Ghana, and Cameroon [12]. The fruit, commonly known in some local communities as "Ube" or "Atili," is valued for its edible pulp. However, processing and consumption of the fruit generate substantial quantities of hard shells, which are commonly discarded as agricultural waste [13]. The accumulation and inappropriate disposal of these shells can contribute to environmental pollution and the inefficient utilization of an otherwise potentially valuable biomass resource. Given their availability and carbon-rich nature, African elemi shells represent a promising but relatively underutilized feedstock for the production of hydrochar through hydrothermal carbonization.

The conversion of African elemi shells into hydrochar therefore provides an opportunity to simultaneously address biomass waste management and the development of sustainable carbon materials. Such valorization can reduce the environmental problems associated with indiscriminate disposal of agricultural residues while creating a useful material with potential applications in carbon capture and other environmental technologies. Furthermore, utilizing a locally available biomass resource can contribute to the development of low-cost and renewable alternatives to conventional carbonaceous adsorbents, thereby supporting broader efforts toward sustainable resource utilization and climate-change mitigation.

In the present study, African elemi shells were utilized as the feedstock for hydrochar production through the hydrothermal carbonization (HTC) process. The effects of key operating parameters on hydrochar production were systematically investigated, with particular attention given to hydrochar yield and textural characteristics, including pore development and surface properties. The adsorption performance of the produced hydrochar toward carbon dioxide (CO_2) was also evaluated to determine its suitability for carbon capture applications. The study is therefore aimed at establishing the potential of African elemi shell as a locally available biomass resource for producing effective carbonaceous adsorbents while providing a sustainable approach to agricultural waste valorization and environmental management. African Elemi (*Canarium schweinfurthii*) can be seen in Figure 1.



Figure 1. African Elemi (*Canarium schweinfurthii*)

2. Method

African elemi shells (*Canarium schweinfurthii*) were obtained from agricultural waste sites in Aku, Igbo Etiti Local Government Area, Enugu State, Nigeria. The shells were washed thoroughly to remove adhering dirt and extraneous materials and then sun-dried for 72 h. The dried shells were crushed into smaller pieces and subjected to chemical pretreatment by soaking in 4 g/dm^3 NaOH solution for 72 h to facilitate the removal of pigments and other impurities. Following pretreatment, the shells were washed repeatedly with water and sun-dried for an additional 72 h. The dried material was subsequently pulverized using an industrial ball mill and sieved to obtain a uniform particle size of approximately 300 μm. The resulting shell powder was collected, and

© 2026 The Author(s)
This work is licensed under a Creative Commons Attribution-ShareAlike 4.0 International License
ISSN: 3110-1577

a 50 g portion was weighed and stored for subsequent hydrothermal carbonization (HTC). This pretreatment procedure provided a relatively homogeneous feedstock with reduced impurities, suitable for the HTC process.

2.1. Research Design for HTC of Hydro-Char

2.1.1. Production of hydrochar from African elemi shell

Hydrochar was produced from the pretreated African elemi shell using hydrothermal carbonization (HTC) under the experimental conditions defined by the design matrix. For each run, 50 g of biomass was mixed with the required volume of water to achieve the specified water-to-biomass (W/B) ratio and loaded into a sealed hydrothermal reactor. The reactor was then heated to the prescribed reaction temperature and maintained at the selected residence time at a controlled heating rate. After completion of the reaction, the reactor was cooled to ambient conditions before the solid and liquid products were separated. The recovered hydrochar was thoroughly washed with water to remove residual soluble and water-soluble compounds and subsequently sun-dried for 72 h. The dried hydrochar was collected and retained for further analysis. The procedure was repeated for the experimental conditions specified in the design matrix, with particular variation in reaction temperature and residence time.

2.1.2. Research Design for Hydro-Char Production

The hydrothermal carbonization (HTC) experiments were designed and optimized using Response Surface Methodology (RSM) based on a Central Composite Design (CCD). Design-Expert software (Version 13) was used to evaluate the influence of reaction temperature, reaction time, and water-to-biomass (W/B) ratio on the selected process responses. The responses considered were char yield, oil yield, specific surface area, pore volume, and pore size. A total of 15 experimental runs comprising different combinations of the process variables were generated and evaluated to establish the relationships between the operating conditions and the resulting hydrochar properties. Table 1 shown a Design factors and their maximum and minimum values for HTC.

Table 1. Design factors and their maximum and minimum values for HTC

Factor	Name of factor	Unit	minimum level	maximum level
A	Reaction Temperature	°C	180.00	220.00
B	W-B Ratio	g	8.00	12.00
C	Reaction Time	min	30.00	90.00

2.2. Research Design Response Analysis

The textural properties of the hydrochars were characterized by nitrogen adsorption–desorption analysis using a Gemini Surface Area Analyzer (Micromeritics, USA), following the Brunauer–Emmett–Teller (BET) approach. Approximately 0.15 g of each hydrochar sample was vacuum-degassed at 250 °C prior to analysis to remove moisture and other adsorbed species [14]. Nitrogen adsorption–desorption measurements were subsequently performed at liquid nitrogen temperature. The specific surface area, total pore volume, and pore size distribution were determined from the adsorption data using the BET and Barrett–Joyner–Halenda (BJH) models. The BET surface area was evaluated within a relative pressure range of 0–0.38, while the BJH method was applied to assess the mesopore distribution within the 2–50 nm pore-size range. The hydrochar exhibiting the highest specific surface area and favourable pore characteristics was selected as the most suitable sample for subsequent CO_2 adsorption studies.

2.2.1. Analysis of the Results

The hydrochar yield obtained from each experimental run was determined gravimetrically using a digital weighing balance and reported as a percentage of the initial dry biomass mass. Following the HTC process, the recovered and dried hydrochar was weighed, and the yield was calculated using the standard relationship commonly adopted for hydrothermal carbonization studies, as expressed in the Equation (1), Equation (2), Equation (3) below, and Table 2 shown a HTC Research Design Factors and Responses.

$$\%\, Yield_{HC} = \frac{Mass\ of\ hydro{-}char}{Mass\ of\ Biomass} \times 100 \quad (1)$$

$$\%\, Yield_{BO} = \frac{Mass\ of\ Bio{-}Oil}{Mass\ of\ Biomass} \times 100 \quad (2)$$

$$\%\, Yield_{gas\&water} = 100\% - \%Yield_{BO} - \%Yield_{HC} \quad (3)$$

Where $\%Yield_{HC}$, $\%Yield_{BO}$, $\%Yield_{gas\ \&\ water}$

© 2026 The Author(s)
This work is licensed under a Creative Commons Attribution-ShareAlike 4.0 International License
ISSN: 3110-1577

Table 2. HTC Research Design Factors and Responses

std	Reaction Temperature (°C)	Residence Time (min)	W-B Ratio (g)	Surface Area (m^2/g)	Pore size (nm)	Pore Volume (cc/g)
1	180	30	8	171.82	1.74	0.14
2	220	30	8	580.36	2.34	0.28
3	180	90	8	290.51	2.01	0.16
4	220	90	8	943.36	2.44	0.33
5	180	30	12	248.82	1.78	0.15
6	220	30	12	727.2	2.59	0.3
7	180	90	12	324.82	2.09	0.16
8	220	90	12	1073.93	2.47	0.35
9	166.4	60	10	200.81	1.93	0.15
10	233.6	60	10	735.08	2.48	0.31
11	200	9.5	10	183.93	1.89	0.15
12	200	110.5	10	691.83	2.4	0.3
13	200	60	6.6	508.61	2.26	0.2
14	200	60	13.4	613.03	2.37	0.23
15	200	60	10	484.58	2.28	0.19
16	200	60	10	614.9	2.36	0.22
17	200	60	10	387.42	2.16	0.17
18	200	60	10	654.56	2.44	0.25
19	200	60	10	538.66	2.33	0.2
20	200	60	10	713.27	2.38	0.22

2.3. Hydrochar Characterization Techniques

2.3.1. Elemental Analysis

The elemental composition of the hydrochar was determined to evaluate its chemical characteristics and degree of carbonization. Nitrogen content was quantified using the Kjeldahl method, while carbon, hydrogen, and sulfur concentrations were measured with a LECO CHNS 628 elemental analyzer in accordance with ASTM D5373. Oxygen content was estimated by difference from the measured elemental constituents. The atomic H/C and O/C ratios were subsequently calculated to assess changes in the degree of carbonization and oxygenation of the hydrochar. In addition, the inorganic elemental composition was characterized using an energy-dispersive X-ray fluorescence (EDXRF) ARL QUANT'X Analyzer.

2.3.2. Moisture Content of the Samples

Moisture content was determined using the oven-drying method. Finely ground hydrochar samples were placed in pre-weighed stainless-steel containers and dried in a Memmert oven at 105 °C. Following drying, the containers were removed, cooled to room temperature, and weighed. The drying and weighing procedure were repeated until a constant mass was obtained, indicating the removal of moisture. Each determination was conducted in replicate, and the mean value obtained from the constant masses was used for subsequent analysis (Equation 4).

$$\text{Moisture content (\%)} = \frac{Wi - Wf}{Wi} \times 100 \quad (4)$$

Where Wi = initial mass of the sample, Wf = final mass of the sample after drying.

2.3.3. Volatile Matter of the samples

Volatile matter content was determined using the Meynell method. The moisture-free hydrochar samples obtained from the preliminary drying step were heated at 280 °C for 2 h to facilitate the release of volatile constituents. The samples were subsequently heated at 450 °C for an additional 2 h to complete the oxidation of the remaining combustible matter and promote ash formation. After cooling to room temperature, the residual mass was measured, and the volatile matter content was calculated from the corresponding mass loss can be seen in Equation (5) and Equation (6).

$$\text{Volatile Matter} = W_{\text{initial}} - W_{\text{after heating}} \quad (5)$$

$$\%\ \text{Volatile Matter} = \frac{Wrd - Wds}{Wst} \times 100 \quad (6)$$

© 2026 The Author(s)
This work is licensed under a Creative Commons Attribution-ShareAlike 4.0 International License
ISSN: 3110-1577

Where Wrd = mass due to removal of the volatile matter, Wds = mass of dry sample after heating, Wst = mass of dry sample collected

2.3.4. Ash Content of the samples.

Ash content was determined by heating 1 g of each dried hydrochar sample in a furnace at 630 °C for approximately 1 h. After heating, the samples were transferred to a desiccator and allowed to cool to room temperature before weighing. The procedure was repeated for all samples, and the mean residual mass obtained after cooling was used to determine the ash content can be seen in Equation (7).

$$\text{Ash content } (\%) = \frac{\text{Wa}}{\text{Wi}} \times 100 \tag{7}$$

Where, Wa = mass of the ash, Wi = initial mass of dried sample.

2.3.5. Fixed Carbon Content of the samples

The fixed carbon content of the hydrochar was determined by difference from the measured moisture, volatile matter, and ash contents. Fixed carbon represents the non-volatile carbonaceous residue that remains after the release of volatile constituents during thermal decomposition [13]. The fixed carbon content was calculated using the following equation:

$$\text{Fixed carbon content } (\%) = 100\% - (\%\text{AC} - \%\text{VM} - \%\text{MC}) \tag{8}$$

Where, AC = Ash content, VM = Volatile Matter, MC = Moisture Content.

2.3.6. H/C and O/C Ratio

The carbon, hydrogen, and oxygen contents of the African elemi shell, hydrochar, and activated hydrochar were determined using CHNSO elemental analysis. The measured elemental compositions were subsequently used to calculate the hydrogen-to-carbon (H/C) and oxygen-to-carbon (O/C) molar ratios, which provide useful indicators of the extent of carbonization and changes in the oxygenated functional groups of the materials. The molar ratios were calculated using Equations (8) and (9), following the approach [13].

$$\text{H/C} = \frac{\text{Percentage Weight of Hydrogen} \Big/ \text{Molar Weight of Hydrogen}}{\text{Percentage Weight of Carbon} \Big/ \text{Molar Weight of Carbon}} \tag{9}$$

$$\text{O/C} = \frac{\text{Percentage Weight of Oxygen} \Big/ \text{Molar Weight of Oxygen}}{\text{Percentage Weight of Carbon} \Big/ \text{Molar Weight of Carbon}} \tag{10}$$

3. Results and Discussion

3.1. Result of the Hydr-ochar Production

Hydrochar samples, with the corresponding production results given in Table 2. The textural properties varied markedly with the HTC conditions. The maximum surface area (1073.93 m^2/g) and pore volume (0.35 cm^3/g) were achieved at 220 °C, 90 min, and 12 g water, while the minimum values of 171.82 m^2/g and 0.14 cm^3/g were obtained at 180 °C, 30 min, and 8 g water. These results indicate that increased reaction severity favoured the development of a more porous hydrochar structure.

3.2. Result of the variables on surface area

3.2.1. Result of reaction temperature & residence time with specific surface area

Figure 2 illustrates the combined influence of reaction temperature and residence time on the specific surface area of the hydrochar. The response surface indicates that increasing reaction temperature generally enhanced the development of surface area, while residence time also contributed to the observed variation. The stronger response associated with temperature suggests that it was the more influential parameter within the investigated range. Increasing the severity of HTC promotes hydrolysis, dehydration, decarboxylation and restructuring of the biomass matrix, thereby facilitating the development of accessible pores. The experimental results support this trend, with a specific surface area of 1073.93 m^2/g obtained at 220 °C and 90 min. The increase in surface area at higher reaction severity indicates more extensive transformation of the original

© 2026 The Author(s)
This work is licensed under a Creative Commons Attribution-ShareAlike 4.0 International License
ISSN: 3110-1577

biomass structure and improved development of adsorption sites. This characteristic is particularly desirable for applications involving CO_2 adsorption.

3.2.2. Effect Reaction of temperature and W-B ratio with surface area

Figure 3 presents the combined effect of reaction temperature and water-to-biomass (W-B) ratio on the specific surface area of the hydrochar. The response surface suggests that reaction temperature exerted a more pronounced influence on surface-area development than the W-B ratio. Increasing temperature enhances the degradation of cellulose, hemicellulose and other thermally susceptible components, while promoting condensation and restructuring of the remaining carbonaceous matrix. The W-B ratio also affects the hydrothermal reaction environment by controlling water availability for hydrolysis and dissolution reactions, although its influence appears comparatively moderate within the investigated range. The highest experimental surface area of 1073.93 m^2/g was obtained under the combined conditions of 220 °C and a W-B ratio of 12. These results demonstrate that reaction temperature was a major determinant of hydrochar textural development, while adjustment of the W-B ratio provided additional control over the resulting surface characteristics.

3.2.3. Effect of residence time and W-B ratio with surface area

Figure 4 shows the interaction between residence time and W-B ratio on the specific surface area of the hydrochar. Both parameters influenced surface area development, although their effects were less pronounced than that of reaction temperature. Increasing residence time provides additional opportunity for hydrolysis, decomposition and reorganization of the biomass constituents, which can progressively expose and develop pore structures. Similarly, increasing the W-B ratio can enhance contact between the biomass and the hydrothermal medium, thereby facilitating the dissolution of susceptible organic components and subsequent structural rearrangement. The experimental data show that prolonged treatment at a higher W-B ratio was associated with improved textural properties, with the highest surface area of 1073.93 m^2/g recorded at 90 min and a W-B ratio of 12. Thus, although neither parameter appears to dominate the response to the same extent as temperature, their combined effect contributes to the development of a more accessible hydrochar structure.

3.3. Effect of the factors on Pore Volume

3.3.1. Effect of Reaction Temperature and Residence Time on Pore Volume

Figure 5 depicts the combined effects of reaction temperature and residence time on the pore volume of the hydrochar. The response surface indicates that pore volume generally increased with increasing reaction severity, with temperature producing a noticeable influence on pore development. Elevated temperatures promote the breakdown of the biomass matrix and facilitate the removal of volatile and soluble constituents, creating additional void spaces within the carbonaceous structure. Residence time further influences this transformation by allowing the hydrothermal reactions to proceed for longer periods. The experimental results confirm the development of pore volume under severe HTC conditions, with a maximum value of 0.35 cm^3/g obtained at 220 °C and 90 min. The increase in pore volume indicates progressive modification of the biomass structure and formation of more accessible internal spaces, which can favour the diffusion and adsorption of CO_2 molecules.

3.3.2. Effect of Reaction Temperature and W-B Ratio on Pore Volume

Figure 6 illustrates the interaction between reaction temperature and W-B ratio on the pore volume of the hydrochar. Reaction temperature appears to exert a stronger influence on pore-volume development, while the W-B ratio produces a comparatively smaller variation. Increasing temperature enhances hydrolysis and degradation of the biomass constituents, followed by condensation and carbonization reactions that modify the internal structure of the hydrochar. The availability of water also affects the reaction medium and the extent of biomass dissolution, although its contribution to pore development is dependent on the applied temperature. The highest experimental pore volume of 0.35 cm^3/g was obtained at 220 °C and a W-B ratio of 12. The results therefore suggest that temperature is particularly important in promoting the formation of accessible pore spaces, while the W-B ratio provides a secondary means of controlling the hydrochar texture.

3.3.3. Effect of Residence Time and W-B Ratio on Pore Volume

Figure 7 presents the combined influence of residence time and W-B ratio on hydrochar pore volume. The response surface shows that both variables contribute to pore development, although their individual effects are comparatively moderate. Longer residence times allow hydrothermal reactions to continue, promoting further decomposition and restructuring of the biomass matrix. Increasing the W-B ratio may also improve the interaction between water and biomass, facilitating hydrolysis and dissolution of susceptible components. The experimental results indicate that the maximum pore volume of 0.35 cm^3/g was achieved at 90 min and a W-B

© 2026 The Author(s)
This work is licensed under a Creative Commons Attribution-ShareAlike 4.0 International License
ISSN: 3110-1577

ratio of 12. The observed increase in pore volume under these conditions suggests that prolonged treatment combined with adequate water availability favours the development of accessible pore structures.

3.4. Effect of the factors on Pore Volume

3.4.1. Effect of Reaction Temperature and Residence Time on Pore Size

Figure 8 illustrates the combined effects of reaction temperature and residence time on the pore size of the hydrochar. The response surface Figure 8a indicates that reaction temperature exerted a more noticeable influence on pore size than residence time. An increase in temperature generally promoted changes in the pore structure as the biomass constituents underwent progressive hydrolysis, dehydration, decarboxylation, and structural rearrangement during HTC. These transformations can modify the accessibility and dimensions of the pores formed within the hydrochar. Residence time also contributed to pore development, with prolonged treatment allowing further decomposition of thermally unstable components and restructuring of the carbon matrix. The profile plot in Figure 8b shows the variation in pore size across the investigated temperature and residence-time ranges, indicating that suitable combinations of these factors are important for controlling the resulting pore structure. The observed changes in pore size are relevant to adsorption performance because pore dimensions influence the accessibility of adsorbate molecules to the internal surface of the hydrochar.

3.4.2. Effect of Reaction Temperature and Water to Biomass Ratio on Pore Size

Figure 9 presents the interaction between reaction temperature and water-to-biomass (W-B) ratio on the pore size of the hydrochar. As shown in Figure 9a, reaction temperature produced a stronger change in pore size, whereas the effect of the W-B ratio was comparatively less pronounced. Increasing temperature enhances the conversion of the biomass matrix and promotes the removal of volatile and oxygen-containing components, thereby altering the pore network and its dimensions. The W-B ratio may also influence the reaction environment by affecting the availability of water for hydrolysis and other HTC reactions, although its effect on pore size appears relatively limited compared with temperature. The profile plot in Figure 9b demonstrates the combined response of pore size to these two variables. The results suggest that reaction temperature is an important operating parameter for regulating pore characteristics, while the W-B ratio provides additional control over the development of the hydrochar structure.

3.4.3. Effect of Residence Time and Water to Biomass Ratio on Pore Size

Figure 10 shows the combined effects of residence time and water-to-biomass (W-B) ratio on hydrochar pore size. The response surface in Figure 10a indicates that both variables influenced the pore characteristics, although their effects were less pronounced than that of reaction temperature. Increasing residence time provides additional opportunity for the degradation and reorganization of the biomass components, which can modify the size and distribution of pores within the hydrochar. Similarly, changes in the W-B ratio alter the reaction medium and may affect the extent of hydrolysis and dissolution of biomass constituents. The profile plot in Figure 10b further illustrates the variation in pore size resulting from the interaction of these factors. The relatively gradual response suggests that residence time and W-B ratio have a moderate influence on pore size, with their combined effect contributing to the adjustment of the hydrochar pore structure. These findings indicate that appropriate control of the HTC conditions is necessary to obtain pore characteristics suitable for adsorption applications.

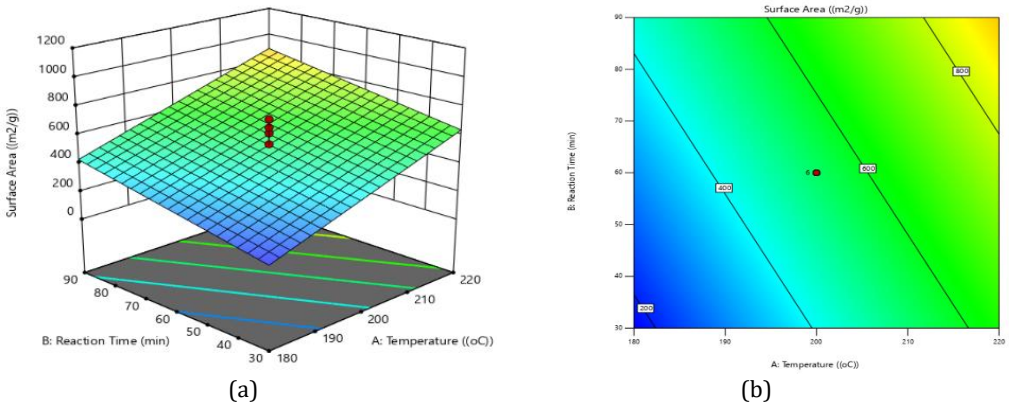

(a) (b)

Figure 2. (a) response surface diagram and (b) profile plot of reaction temperature and residence time on the surface area of char

© 2026 The Author(s)
This work is licensed under a Creative Commons Attribution-ShareAlike 4.0 International License
ISSN: 3110-1577

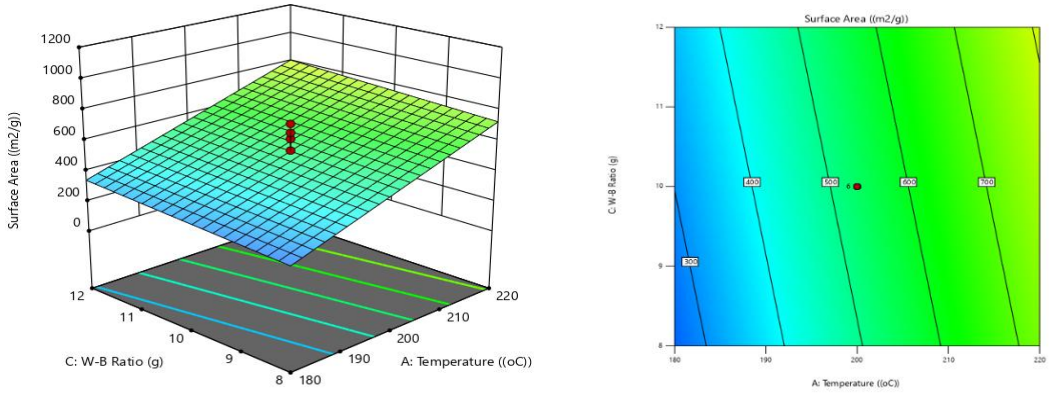

(a) (b)

Figure 3. (a) response surface diagram and (b) profile plot of reaction temperature and water-biomass ratio on the surface area

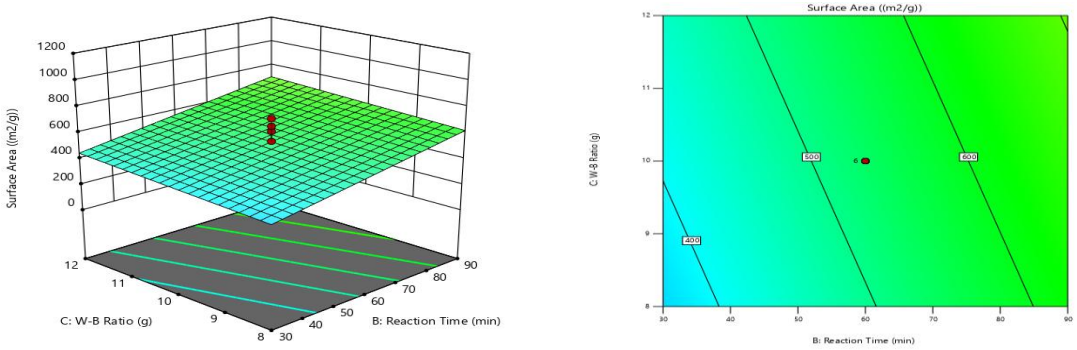

(a) (b)

Figure 4. (a) response surface diagram and (b) profile plot of residence time and water-biomass ratio on surface area

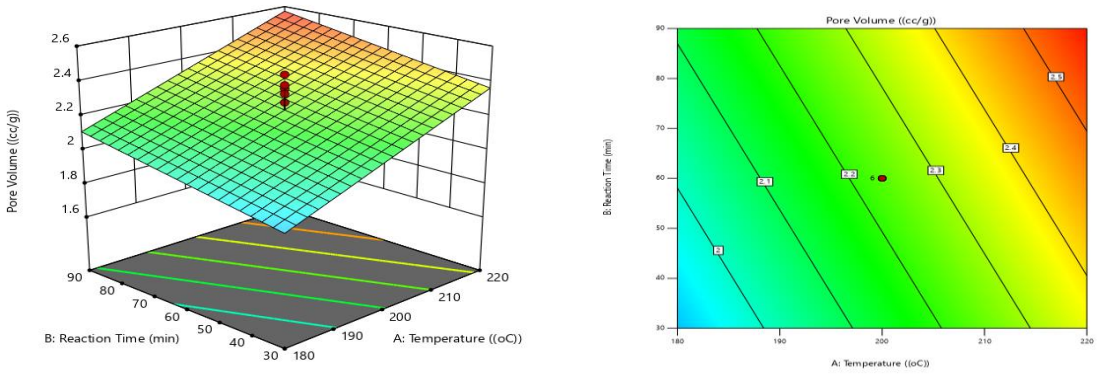

(a) (b)

Figure 5. (a) response surface diagram and (b) profile plot of temperature and residence time on the pore volume

© 2026 The Author(s)
This work is licensed under a Creative Commons Attribution-ShareAlike 4.0 International License
ISSN: 3110-1577

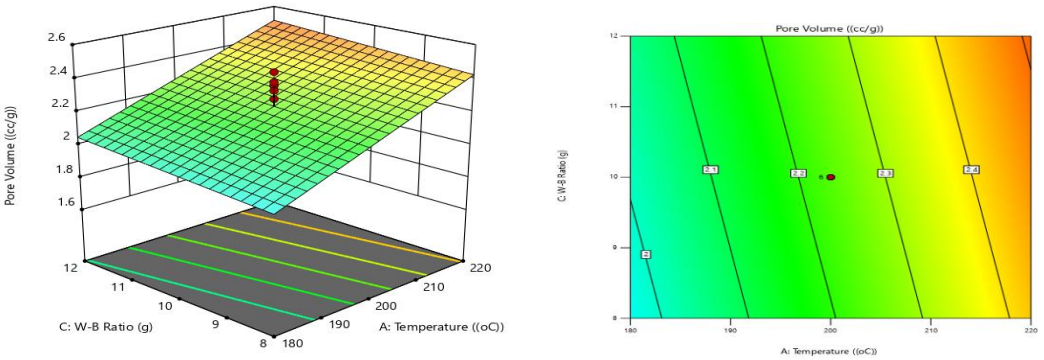

(a) (b)

Figure 6. (a) response surface diagram and (b) profile plot of temperature and water-biomass ratio on the pore volume

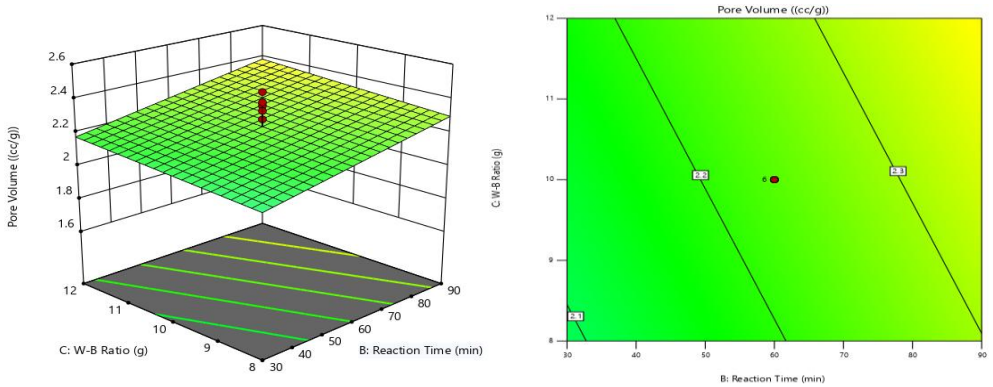

(a) (b)

Figure 7. (a) response surface diagram and (b) profile plot of residence time and water-biomass ratio on the pore volume

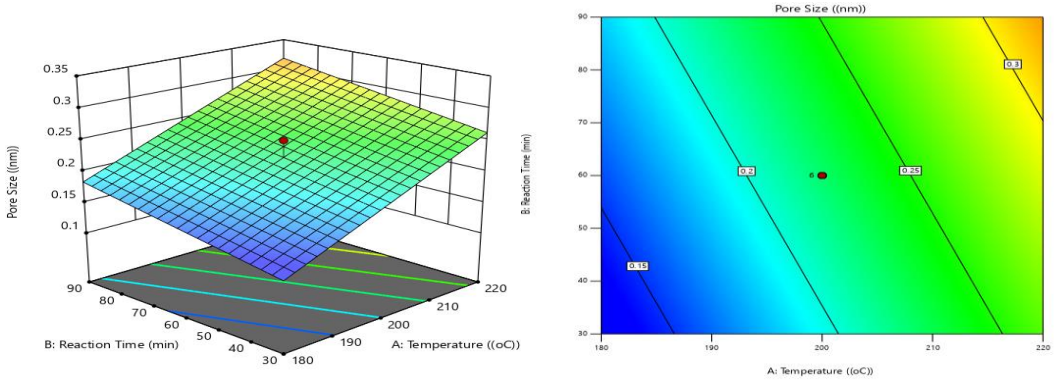

(a) (b)

Figure 8. (a) response surface diagram and (b) profile plot of temperature and residence time on the pore size

© 2026 The Author(s)
This work is licensed under a Creative Commons Attribution-ShareAlike 4.0 International License
ISSN: 3110-1577

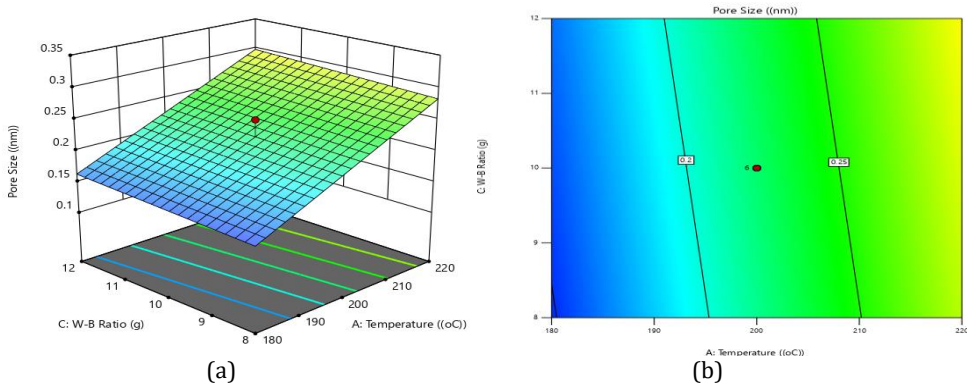

(a) (b)

Figure 9. (a) response surface diagram and (b) profile plot of temperature and water-biomass ratio on the pore size

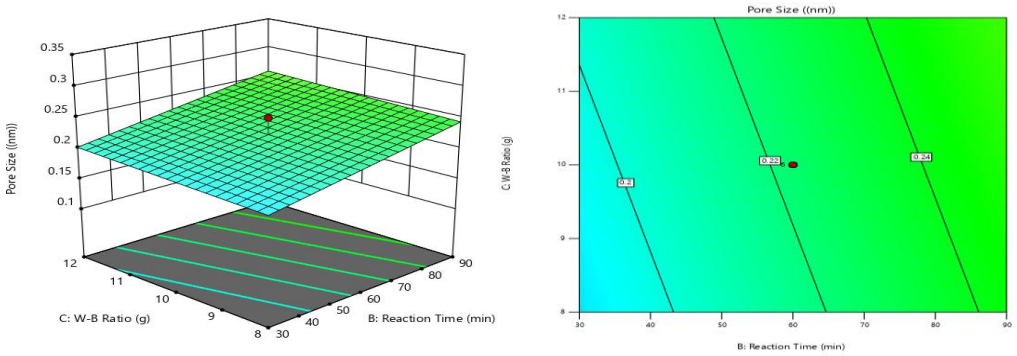

(a) (b)

Figure 10. (a) response surface diagram and (b) profile plot of residence time and water-biomass ratio on the pore size

3.5. Characterization of AES and produced hydrochar

3.5.1. Comparative Analysis of Ultimate and Proximate Results

Ultimate and proximate analyses were performed to characterize the chemical and physicochemical properties of the African elemi shell (AES) and the resulting hydrochar (AESH). Ultimate analysis was used to determine the elemental composition, including carbon, hydrogen, nitrogen, sulfur, and oxygen, together with the corresponding atomic H/C and O/C ratios. Proximate analysis was conducted to evaluate moisture, ash, volatile matter, and fixed carbon contents. The results of these analyses are presented in Figure 11.

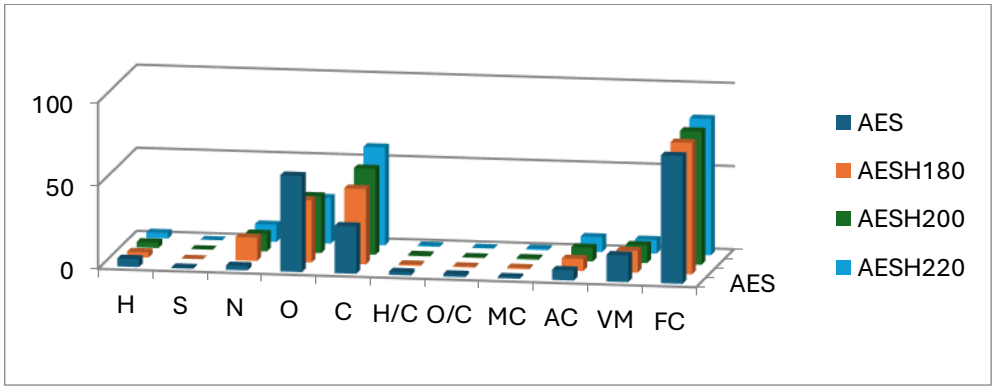

Figure 11. Comparison of the samples Ultimate and Proximate Analysis

© 2026 The Author(s)
This work is licensed under a Creative Commons Attribution-ShareAlike 4.0 International License
ISSN: 3110-1577

Ultimate Analysis

The ultimate analysis showed clear changes in the elemental composition of the African elemi shell (AES) following hydrothermal carbonization. The AESH220 sample produced at 220 °C for 90 min exhibited the highest carbon content, whereas the untreated AES recorded the lowest. The increase in carbon concentration with increasing HTC temperature can be associated with dehydration and polymerization reactions that progressively enrich the solid product in carbon. Conversely, oxygen content decreased as the reaction temperature increased, with the raw AES exhibiting the highest oxygen concentration. These changes indicate progressive transformation of the biomass into a more carbonaceous structure during HTC.

Proximate Analysis

The proximate and ultimate analysis results presented in Table 3 and Fig. 10 demonstrate the changes in the physicochemical composition of AES following HTC. Moisture content was highest in the raw AES and generally decreased after carbonization, although a slight increase was observed at the higher HTC temperature. Ash content increased with increasing reaction temperature, while volatile matter decreased. The reduction in volatile matter indicates progressive decomposition and removal of thermally labile components during HTC, accompanied by greater retention of carbon in the resulting hydrochar. The observed increase in fixed carbon further confirms the conversion of the biomass into a more carbon-rich and thermally stable material.

Surface morphologies and textural characterization

The SEM images in Figure 12 and Table 3 show clear morphological changes in AES following HTC. Raw AES exhibited a rough, fractured and fibrous surface, while AESH180 showed a more porous and aggregated structure. At 220 °C, the hydrochar developed a denser and more fractured carbonaceous surface, indicating greater structural transformation. EDS analysis confirmed carbon enrichment, with carbon increasing from 54.79% in raw AES to 85.27% and 88.27% in AESH180 and AESH220, respectively. Conversely, nitrogen decreased from 42.30% to 14.19% and 10.88%. These changes demonstrate progressive carbonization and removal of nitrogen-containing and other soluble constituents as HTC temperature increased.

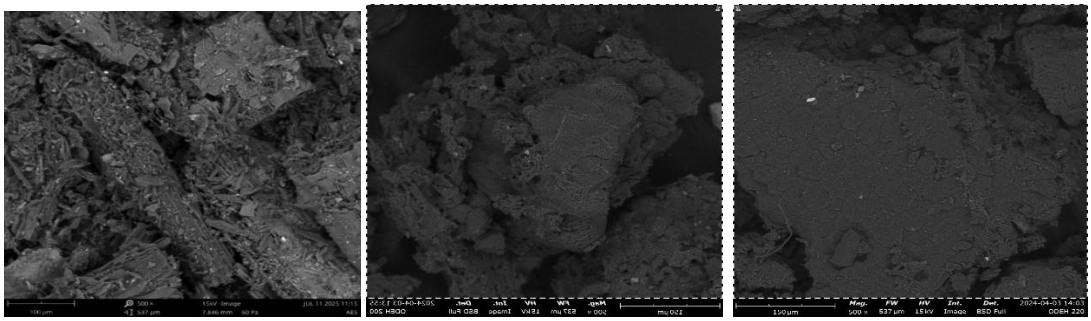

(a) (b) (c)

Figure 12. Comparison of the samples' SEM at 220 °C and 180 °C

Table 3. Comparison of the samples' SEM at 220 °C and 180 °C

Element Number	Element Symbol	Element Name	Atomic Conc.	Weight Conc.
6	C	Carbon	88.27	85.80
7	N	Nitrogen	10.88	12.34
11	Na	Sodium	0.60	1.12
26	Fe	Iron	0.10	0.45
12	Mg	Magnesium	0.15	0.30
14	Si	Silicon	0.00	0.00
13	Al	Aluminium	0.00	0.00
16	S	Sulfur	0.00	0.00
17	Cl	Chlorine	0.00	0.00
22	Ti	Titanium	0.00	0.00
20	Ca	Calcium	0.00	0.00
19	K	Potassium	0.00	0.00
15	P	Phosphorus	0.00	0.00

3.5.2. FTIR analysis of AESH

Figure 13Figure 13 shows the FTIR spectrum, which indicates that hydrothermal treatment at 220 °C caused significant transformation of the biomass structure. The broad band around 3348.37 cm^{-1} is associated with O - H stretching, while the region around 2900 cm^{-1} represents aliphatic C–H groups. Absorptions around 1636.17 cm^{-1} indicate carbonyl and/or aromatic C=C groups, whereas bands between 1123.4 cm^{-1} are mainly associated with C–O vibrations. The reduced intensity of these bands suggests dehydration, decarboxylation and

© 2026 The Author(s)
This work is licensed under a Creative Commons Attribution-ShareAlike 4.0 International License
ISSN: 3110-1577

aromatization during hydrothermal carbonization, resulting in a more carbon-rich hydrochar. The remaining oxygen-containing functional groups may contribute to its potential CO_2 adsorption capacity.

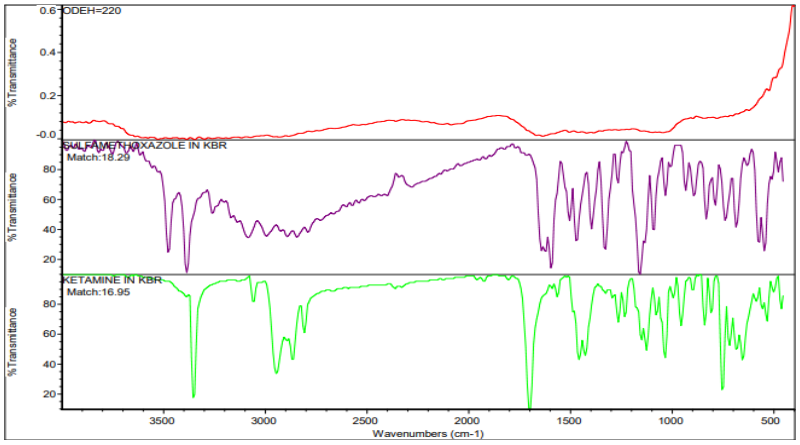

Figure 13. FTIR spectra of AESH.

3.5.3. Thermogravimetric analyses of AESH

Figure 14a and Figure 14b present the TGA/DTA profiles of AES and AESH. Both samples exhibited an initial mass loss of approximately 2–3%, corresponding to moisture removal. The major thermal decomposition occurred between 300 and 500 °C. AES showed a predominantly single-stage degradation with a maximum rate near 400 °C, whereas AESH exhibited a multi-stage decomposition pattern around 330–350 °C, indicating changes in its thermal degradation behaviour after HTC. The final residue was approximately 26% for AES and 13.6% for AESH, suggesting differences in their inorganic and thermally stable fractions. The DTA profiles supported these observations, confirming the distinct degradation pathways of the raw biomass and hydrochar [6].

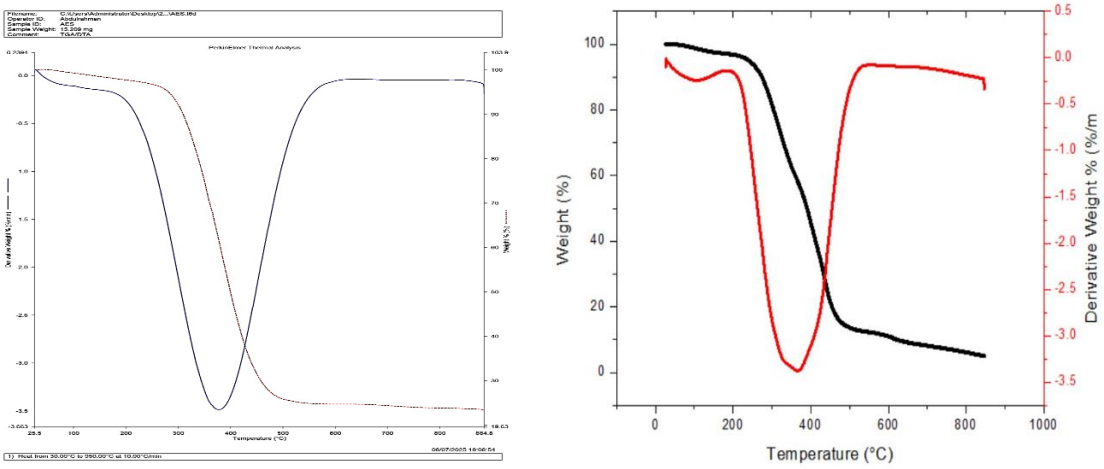

a) b)

Figure 14. a) TGA/DTA curve of AES; b) TGA/DTA curve of AESH.

4. Conclusion

This study investigated the conversion of African elemi shell (AES), an underutilized agricultural residue, into value-added hydrochar and biofuel through hydrothermal carbonization (HTC). The process transformed the biomass into a carbon-rich material with enhanced surface characteristics and potential for CO_2 adsorption. The hydrochar exhibited a developed porous structure, relatively high surface area, and functional groups that can contribute to gas adsorption. HTC experiments were conducted in a stainless-steel autoclave under controlled temperature and pressure conditions, with an optimum condition of approximately 220 °C and 65 min identified based on the combined surface and pore characteristics of the hydrochar. Characterization using SEM–EDS, TGA/DTA, proximate analysis, and ultimate analysis confirmed substantial changes in morphology, elemental composition, and thermal behaviour following HTC. The findings demonstrate that AES can serve as a promising renewable feedstock for producing carbonaceous materials with potential applications in CO_2 capture, energy conversion, and other environmental technologies.

© 2026 The Author(s)
This work is licensed under a Creative Commons Attribution-ShareAlike 4.0 International License
ISSN: 3110-1577

Author Contributions

All authors have equal contributions to the paper. All the authors have read and approved the final manuscript.

Funding

No funding support was received.

Declaration of Conflicting Interests

The author declared no potential conflicts of interest with respect to the research, authorship, and/ or publication of this article.

Data Availability

The datasets generated during and/ or analysed during the current study are available from the corresponding author on reasonable request.

Declaration on AI Use

The authors declare that no artificial intelligence (AI) or AI-assisted tools were used in the preparation of this manuscript.

References

[1] P. Smith, J.-F. Soussana, D. Angers, L. Schipper, C. Chenu, D. P. Rasse, N. H. Batjes, F. van Egmond, S. McNeill, M. Kuhnert, C. Arias-Navarro, J. E. Olesen, N. Chirinda, D. Fornara, E. Wollenberg, J. Álvaro-Fuentes, A. Sanz-Cobena, and K. Klumpp, "How to measure, report and verify soil carbon change to realize the potential of soil carbon sequestration for atmospheric greenhouse gas removal," *Global Change Biology*, vol. 26, no. 1, pp. 219–241, 2019, doi: 10.1111/gcb.14815.

[2] W. Liu, G. Wang, M. Yu, H. Chen, Y. Jiang, M. Yang, and Y. Shi, "Projecting the future vegetation-climate system over East Asia and its RCP-dependence," *Climate Dynamics*, vol. 55, no. 9, pp. 2725–2742, 2020, doi: 10.1007/s00382-020-05411-2.

[3] Y. Zhang, Z. Jin, and M. Sikand, "The top-of-atmosphere, surface and atmospheric cloud radiative kernels based on ISCCP-H datasets: Method and evaluation," *Journal of Geophysical Research: Atmospheres*, vol. 126, no. 24, Art. no. e2021JD035053, 2021, doi: 10.1029/2021JD035053.

[4] W.-T. Chen, Y. Zhang, T. H. Lee, Z. Wu, B. Si, C.-F. F. Lee, A. Lin, and B. K. Sharma, "Renewable diesel blendstocks produced by hydrothermal liquefaction of wet biowaste," *Nature Sustainability*, vol. 1, pp. 702–710, 2018, doi: 10.1038/s41893-018-0172-3.

[5] C. Goel, S. Mohan, and P. Dinesha, "CO_2 capture by adsorption on biomass-derived activated char: A review," *Science of the Total Environment*, vol. 798, Art. no. 149296, 2021, doi: 10.1016/j.scitotenv.2021.149296.

[6] Z. Li, W. Yi, Z. Li, C. Tian, P. Fu, Y. Zhang, L. Zhou, and J. Teng, "Preparation of solid fuel hydrochar over hydrothermal carbonization of red jujube branch," *Energies*, vol. 13, no. 2, Art. no. 480, 2020, doi: 10.3390/en13020480.

[8] Y.-J. Wang, Y. Yu, H.-J. Huang, C.-L. Yu, H.-S. Fang, C.-H. Zhou, X. Yin, W.-H. Chen, and X.-C. Guo, "Efficient conversion of sewage sludge into hydrochar by microwave-assisted hydrothermal carbonization," *Science of the Total Environment*, vol. 803, Art. no. 149874, 2022, doi: 10.1016/j.scitotenv.2021.149874.

[9] J. Fang, B. Gao, J. Chen, and A. R. Zimmerman, "Hydrothermal carbonization for valorizing waste biomass: Role of feedstock properties and reaction conditions on hydrochar structure and adsorption performance," *Bioresource Technology*, vol. 292, Art. no. 121974, 2019, doi: 10.1016/j.biortech.2019.121974.

[10] W. Wang, W.-H. Chen, and M.-F. Jang, "Characterization of hydrochar produced by hydrothermal carbonization of organic sludge," *Future Cities and Environment*, vol. 6, no. 1, Art. no. 13, pp. 1–10, 2020, doi: 10.5334/fce.102.

[11] I. C. Okoro, G. C. Ugochukwu, and M. A. Ezeokonkwo, "Proximate and phytochemical composition of *Canarium schweinfurthii* (African Elemi) pulp and seed," *International Journal of Scientific & Engineering Research*, vol. 8, no. 8, pp. 1504–1508, 2017.

[12] A. A. Adewale, O. Olawale, and A. S. Akinwale, "Nutritional and phytochemical evaluation of African Elemi (*Canarium schweinfurthii*) fruit pulp and seed oil," *Journal of Applied Sciences and Environmental Management*, vol. 23, no. 3, pp. 501–507, 2019, doi: 10.4314/jasem.v23i3.16.

[13] S. Lowell, J. E. Shields, M. A. Thomas, and M. Thommes, *Characterization of Porous Solids and Powders: Surface Area, Pore Size and Density*. Dordrecht, The Netherlands: Springer, 2004, doi: 10.1007/978-1-4020-2303-3.

[14] S. Brunauer, P. H. Emmett, and E. Teller, "Adsorption of gases in multimolecular layers," *Journal of the American Chemical Society*, vol. 60, no. 2, pp. 309–319, 1938, doi: 10.1021/ja01269a023.

© 2026 The Author(s)
This work is licensed under a Creative Commons Attribution-ShareAlike 4.0 International License
ISSN: 3110-1577